Multifunctional ZnO NPs-chitosan-gallic acid hybrid nanocoating to overcome contact lenses associated conditions and discomfort

Javier Hoyo,[a] *Kristina Ivanova,*[a] *Ester Guaus,*[a] *Tzanko Tzanov*[a,*]

a) Grup de Biotecnologia Molecular i Industrial, Department of Chemical Engineering, Universitat Politècnica de Catalunya, Rambla Sant Nebridi 22, 08222, Terrasa, Spain

*Corresponding author: Dr. Tzanko Tzanov, tel.: +34 93 739 85 70, fax: +34 93 739 82 25, e-mail: tzanko.tzanov@upc.edu

Con formato: Fuente: 10 pto

Con formato: Fuente: 10 pto

Con formato: Fuente: 10 pto

ABSTRACT

Contact lenses (CL) provide visual correction but their use may also induce several adverse effects causative of discomfort and conditions that lead to stop or discontinue their use. Discomfort is mainly caused by insufficient wetting, impairment of the antioxidant defence system and eye infections. The current work reports on a single step sonochemical coating of CL with ZnO nanoparticles (NPs), chitosan (CS) and gallic acid (GA). GA and CS are expected to improve the comfort of CL by imparting respectively antioxidant properties and enhanced wettability, while their combination with ZnO NPs provides the CL with antimicrobial properties. The ternary composite coating presents high antibacterial efficiency (> 4.5 logs reduction) against *S. aureus* causative of CL-related conditions, and maintains good biocompatibility (> 72 %) with human cell lines. The obtained multi-functionality on the CL did not affect their geometry and refractive properties.

KEYWORDS: contact lenses, ZnO nanoparticles, chitosan, gallic acid, sonochemistry, antibacterial coating

Abbreviations

Antimicrobial peptides: AMP, Atomic force microscopy: AFM, Chitosan: CS, Contact lenses: CL, Energy-dispersive X-ray spectroscopy EDS, Field emission scanning electron microscopy: FESEM, Gallic acid: GA, Metal oxide: MeO, Nanoparticles: NPs, Reactive oxygen species: ROS, Ultrasound: US, Water contact angle: WCA.

1. INTRODUCTION

Well-performing contact lenses (CL) provide good comfort, physiology and handling, which are achieved through a combination of material characteristics, CL design and manufacturing process. At present, over 50 million people in the USA and nearly 150 million worldwide wear CL [1]. However, more than 25 % of CL wearers experience discomfort and in more than 50 % of these cases, people discontinue wearing CL [2]. The most common causes for discomfort are the insufficient wetting, lubrication and protein adsorption on the ocular surface [3] and a fear of, or history of eye infections [4].

Con formato: Fuente: 10 pto
Con formato: Fuente: 10 pto
Con formato: Fuente: 10 pto
Con formato: Fuente: 10 pto
Con formato: Fuente: 10 pto
Con formato: Fuente: 10 pto
Con formato: Fuente: 10 pto

The healthy eye is constantly wetted by tear film, which lubricates and protects the ocular surface, distribute nutrients, maintain optical clarity, and collect and eliminate wastes. The wearing of CL reduces the tear film function thus altering the native eye environment allowing bacteria to grow and affect the eye health [4]. Microbial contamination of CL is the reason for several eye-related conditions that, besides the discomfort, may cause serious complications resulting in vision loss [5]. The most relevant microbial conditions associated to CL wearing are microbial-associated keratitis (MK), infiltrative keratitis (IK), acute red eye (CLARE) and CLs peripheral ulcer (CLPU) [6]. Gram-positive representatives such as *Staphylococcus aureus* (*S. aureus*) and *Streptococcus pneumonia* are mainly responsible for IK and CLPU, but also involved in MK and CLARE [1,7].

Different antimicrobial approaches were proposed to reduce the high incidence of bacterial infections on medical devices [8]. In particular, CL were coated with antimicrobial peptides (AMPs) [9] with a broad spectrum biocidal activity. However, the use of AMPs is limited due to their elevated cost and low functional stability *in vivo* [10]. The impregnation of CL with nonsteroidal anti-inflammatory drugs successfully inhibited the adhesion of bacteria on the CLs surface [11], but the use of these drugs is compromised due to adverse effects [12]. Another more innovative strategy is based on coating the CL with quorum sensing inhibitors [13], but their toxicity and poor stability requires further research. Alternatively, metal and metal-oxide nanoparticles (NPs) have been proposed as antimicrobial agents for bacterial eradication in biomaterials [14]. Silver NPs are the most widely used antimicrobial nano-entities, however, their potential toxicity [14] shifted the attention to zinc oxide (ZnO) NPs with good antimicrobial activity coupled to biocompatibility at low concentration [15–17]. The mechanism of action of ZnO NPs includes formation of reactive oxygen species (ROS) that affect bacterial membrane causing leakage of intracellular components and damage of bacterial proteins and DNA [18,19]. ZnO nano-functionalization of CL would provide them with antimicrobial properties.

The perception of comfort at wearing CL is related to the facile tear film spread and the reduced deposition of proteins and lipids from the tear film on CL surface as a function of the CL wettability [20]. High wettability, additionally, fairly diminishes the CL-related adverse effects, such as reduced vision, inflammatory responses and bacterial colonization [21,22]. Previous works used hydrophilic polymers to functionalize the surface of CL improving their wettability [23,24]. Although chitosan (CS) has been widely studied in the field of biomaterials development because of its biodegradability, biocompatibility

and antibacterial properties [25], only few studies [26,27] have exploited its multiple benefits for reducing protein deposition on biomaterials. Herein, coating the CL with CS will bring about their enhanced wettability and antimicrobial properties. On the other hand, the CS integration with gallic acid (GA) [28] would additionally increase the comfort of the coated CL imparting antimicrobial and antioxidant activities. The human eye is subjected to oxidative stress due to its constant and intense exposure to light, metabolic activity and high oxygen tension. The cornea is the first barrier of the eye to the external environment and presents a robust antioxidant defence system [29]. However, deficiencies or alteration of this system may contribute to pathogenic eye conditions such as cataract, glaucoma, keratoconus and dry eye [29–31].

Surface modification has been recognized as one of the most versatile methods to tailor the properties of materials. Unlike the time-consuming coating procedures using harsh chemicals, high intensity ultrasound (US) has emerged as a straightforward and environmentally friendly approach to functionalize the surface of paper, polymers and textiles [28,32–34]. The coating results from the high-speed microjets generated upon the implosive collapse of bubbles formed in liquid medium under US, i.e. the cavitation phenomenon [35]. These microjets project NPs or molecules found in the vicinity of the collapsing bubbles towards the surface of a solid material of interest forming stable coatings [34].

The current work aims to develop biocompatible and efficient antibacterial coatings on CL that simultaneously confers comfort at wearing and maintain CL optical properties. This will be achieved by the simultaneous deposition of ZnO NPs, CS and GA in a one-step US coating process. These three bioactive compounds will contribute to the antibacterial properties and biocompatibility of the coatings. Additionally, the antioxidant activity of GA coupled to the enhanced wettability conferred by CS would increase substantially the comfort of the CL. The antibacterial efficiency of the coatings will be validated against *S. aureus* causative of CL-related ocular conditions. Additionally, the biocompatibility and optical properties of CL after the coating will be evaluated to verify whether the surface nano-structuring upon exposure to US would not modify the original vision correction properties.

Con formato: Fuente: 10 pto
Con formato: Fuente: 10 pto
Con formato: Fuente: 10 pto
Con formato: Fuente: 10 pto
Con formato: Fuente: 10 pto
Con formato: Fuente: 10 pto
Con formato: Fuente: 10 pto
Con formato: Fuente: 10 pto
Con formato: Fuente: 10 pto
Con formato: Fuente: 10 pto
Con formato: Fuente: 10 pto
Con formato: Fuente: 10 pto
Con formato: Fuente: 10 pto
Con formato: Fuente: 10 pto
Con formato: Fuente: 10 pto
Con formato: Fuente: 10 pto

2. MATERIALS AND METHODS

2.1 Materials, reagents and bacteria

Comfilcon A (silicone-hydrogel) CL - nominal dioptric power (PWR_d) - 7.00 D and nominal water content 48 % - were purchased from Coopervision (USA). Low molecular weight CS with Mw = 15 kDa and 87 % DDA was provided by Kitozyme. Water dispersion of ZnO NPs (20 % (w/v) in H_2O, avg. NP size ≤ 40 nm), GA (≥ 97,5 %), sodium acetate (> 99 %), sodium phosphate (> 99 %), 2,2'-azino-bis(3-ethylbenzothiazoline-6-sulphonic acid) (≥ 98 %, ABTS), Folin-Ciocalteu's phenol reagent (2N), Dulbecco's Modified Eagle Medium (DMEM), plate-count agar and all other reagents for bacterial studies were purchased from Sigma–Aldrich (Spain) unless otherwise specified. *S. aureus* (ATCC 25923) was used in the antibacterial activity assays. Nutrient broth (NB) for bacterial culturing was provided by Sharlab (Spain).

2.2 Sonochemical coating of CL with ZnO NPs, CS and GA

The US coating process was performed using ultrasonic transducer (Ti-horn, 20 kHz, 750 W, Sonics and Materials VC750, USA) for 30 min at 22 ± 1 ºC and 35 % amplitude in a glass vessel containing 50 mL of 0.3 % (w/v) CS, 0.3 % (w/v) GA and/or 0.006 % (v/v) ZnO NPs aqueous solutions as well as one CL. The power and the intensity were 21.5 W and 0.43 W/cm^3, respectively. The reaction composition and samples abbreviations are summarized in Table 1. After the reaction, the CL was thoroughly washed with milliQ water to remove the loosely fixed compounds. Control samples were prepared at the same coating conditions, but in milliQ water without any actives to assess the effect of the US on the CL optical properties.

Table 1. Reaction conditions and samples abbreviations.

Sample abbreviation	ZnO	CS	CS/ZnO	GA	GA/ZnO	CS/GA	CS/GA/ ZnO
Reaction mixture	0.006 % ZnO NPs	0.3 % CS	0.3 % CS 0.006 % ZnO NPs	0.3 % GA	0.3 % GA 0.006 % ZnO NPs	0.3 % CS and 0.3 % GA	0.3 % CS and 0.3 % GA 0.006 % ZnO NPs

2.3 Characterization of CL

Dioptric power of CL

In order to evaluate the PWR_d of coated and control CL, they were dehydrated in a vacuum desiccator (≈ 3 hours) and analysed using the Auto Lensmeter TL-3000B (Tomey Corporation). All results are reported as mean values ± SD (n = 3).

Water content of CL

The coated and control CL were dehydrated in a vacuum desiccator (≈ 3 hours) until no further change in their weight was observed. The water content of the CL was expressed as a percentage according to eq. 1:

$$H\ \% = ((W_h - W_d)/W_d)) \times 100 \qquad (1)$$

where W_h is the weight of the hydrated coated CL after immersing in milliQ water for 24 h, W_d is the weight of the uncoated dried CL and H % is the percentage of water content. All results are reported as mean values ± SD (n = 3).

Water contact angle of CL

The wettability of CL surface was evaluated by advancing water contact angle (WCA) using the sessile drop method using a DSA100 drop shape analyser from KRÜSS GmbH. The measurements were performed at 22 ± 1 ºC and at a relative humidity of 35 ± 2 % as described previously [36]. Briefly, the CL was placed on a lens cleaning tissue to absorb the residual surface liquid, fixed on a holder and then introduced in the drop shape analyser. A 4 µl milliQ water drop controlled by a micrometer pass dosage was dispensed by the tip of the dosing needle and transferred to the CL surface by moving the sample stage upwards the drop, ensuring a total time of exposure of CL to air of 2 min. The process was captured and processed by DSA4 software using tangent method to calculate the WCA. All results are reported as mean values ± SD (n = 3).

Con formato: Fuente: 10 pto

Con formato: Fuente: 10 pto

Surface morphology of the coated CL

The surface morphology and the presence of ZnO NPs in the coatings were studied by field emission scanning electron microscopy (FESEM) JEOL J-7100 with Energy-dispersive X-ray spectroscopy (EDS) detector. The surface topography of the coatings was further assessed by atomic force microscopy (AFM) in liquid tapping mode using a Multimode AFM controlled by Nanoscope IV electronics (Veeco, Santa Barbara, CA) under ambient conditions. Triangular AFM probes with Antimony (n) doped Si cantilevers and silicon tips were used (RTESPA-150, Bruker) with nominal spring constant of 6 N/m and a resonant frequency of 150 kHz. The CL was cut and glued on a polytetrafluoroethylene (PTFE) surface that, in turn, is glued to a metallic AFM disk. Afterward, a drop (20 µL) of milliQ water was placed on the CL and 10 min were lagged for stabilization prior placing the holder in the AFM instrument. After thermal stabilization (10 min), the images were acquired at 1 Hz line frequency and minimum vertical force to reduce sample damage. Nanoscope Analysis v1.5 software was used for image processing.

Zn, CS and GA quantification

Determination of Zn was performed by inductively coupled plasma mass spectrometry (ICP-MS) in a "Perkin Elmer Nexion 350d" instrument under standard conditions. Calibration with five standards was

prepared from certified standard solutions. The amount of ZnO NPs embedded on the coatings was determined after extraction with 1 mL HNO_3 and 1 mL H_2O_2 at 90 ºC for 24 h.

The amount of CS in the ternary CL coating was assessed using fluorescein isothiocyanate (FITC)-labelled CS. Prior to US coating, CS (10 mg/mL) was dissolved in miliQ water and mixed with 1 mg/mL FITC solution, prepared in anhydrous dimethyl sulfoxide, under continuous stirring. For each 1 mL of CS solution 50 µL of FITC were added. The reaction was incubated in the dark at 4 ºC overnight and the unreacted FITC was removed from the FITC-CS conjugate using PD-10 Desalting Columns (GE healthcare). Afterwards, the US coating process was carried out with 0.3 % FITC-CS, 0.3 % GA and 0.006 % ZnO NPs as described above. The fluorescence intensity of the solution containing FITC-CS was measured at Ex/Em (490/525) at the beginning (I_{in}) and the end (I_f) of the reaction using TECAN Infinite M 200. The amount of CS deposited on the CL was calculated from the intensity difference (I_f - I_{in}) using a calibration curve plotted between fluorescence intensity of the FITC-CS and its concentration.

The amount of GA in the ternary CL coating was also determined. The coated CL was immersed in 3 mL miliQ water with pH 10 for 24 h to dissolve/extract the GA. Then, 50 µL of the solution were mixed with 35 µL of 0.2 N Folin-Ciocalteu's reagent, 600 µL of milliQ water and 60 µL 20 % (w/v) sodium carbonate. The samples were placed in a dark for 1 h at room temperature. After, 200 µL of each solution were transferred to a 96-well microplate and the absorbance was recorded at 765 nm. A calibration curve was constructed with GA standard solutions and used to calculate the amount of GA in the coating.

2.4 Bioactivity evaluation

Antioxidant activity

The antioxidant activity of GA containing CL was determined by the DPPH free radical scavenging method. The assay measures spectrophotometrically the decrease of absorbance of the DPPH radical at 517 nm [37]. Briefly, a portion of CL (5 mg) was incubated in 60 µM DPPH solution in methanol at 37 ºC in dark conditions for 30 min, and after removal of the CL, the absorbance at 517 nm was measured (Infinite M200, Tecan, Austria). Eq. 2 was used to calculate the antioxidant activity of the samples,

Con formato: Fuente: 10 pto

Con formato: Fuente: 10 pto

$$\text{DPPH scavenging (\%)} = [1 - (A/A_0)] \times 100, \qquad (2)$$

where A_0 is the absorbance of the negative control (neat DPPH solution) and A is the absorbance of DPPH after incubation with CL. All results are reported as mean values ± SD (n = 3).

Antibacterial activity

The antibacterial activity of CL was assessed as follows: single *S. aureus* colony was transferred from streak agar plate in 5 mL NB and incubated at 37 ºC and 230 rpm overnight. Then, the culture was diluted with sterile PBS solution until $O.D._{600}$ = 0.01. A portion (5 mg) of the coated CL was incubated with 5 mL of the diluted bacterial suspension for 24 h at 37 ºC and 230 rpm. After, the suspensions were serially diluted with sterile PBS solution, plated on the corresponding plate count agar and further incubated at 37 ºC for 24 h to determine the number of survived bacterial colonies. The antibacterial activity is expressed as Log reduction according to the Eq. 3,

$$\text{Log reduction} = \log_{10}(B) - \log_{10}(C) \quad (3),$$

where B and C are the average number of bacterial colony forming units (CFU) per mL at the beginning and after 24 h of incubation with coated CL, respectively. All results are reported as mean values ± SD (n = 3).

Cytotoxicity evaluation

Human foreskin fibroblasts (ATCC®-CRL-4001™, BJ-5ta) and keratinocytes (HaCaT cell line) were used to assess the biocompatibility of the coatings as described previously [38]. The cells were maintained in 4 parts DMEM at 37 °C in a humidified atmosphere with 5 % CO_2. At pre-confluence, the cells were harvested using trypsin-EDTA (ATCC-30-2101) and seeded at a density of 1.2 x 10^5 cells/well. After 24 h, the cells were washed twice with sterile PBS; the CL (5 mg) were placed in the wells and 500 µL of DMEM was added. The cells were incubated at 37 °C for 24 h. Afterward, the samples were removed, the growth media withdrawn and the cells were washed twice with PBS and stained for 4 h at 37 °C with 100 µL 10 % (v/v) AlamarBlue™ Cell Viability Reagent in DMEM. After that, the absorbance at 570 nm was measured in a microplate reader (Infinite M200, Tecan, Austria).

Con formato: Fuente: 10 pto

Con formato: Fuente: 10 pto

3. RESULTS AND DISCUSSION

3.1 Characterization of CL

Commercial CL were sonochemically functionalized with the antimicrobial compounds ZnO NPs, CS and GA. The high intensity US produces a strong cavitation that favours the homogeneity of the NPs solution and simultaneously projects the ZnO NPs, GA and CS towards the CL surface [39]. The lack of aggregation and the uniform distribution of ZnO NPs on CL surface, coupled to their small size and narrow size distribution favours the antimicrobial effect [40]. The presence of CS and GA is anticipated to improve the comfort of CL by conferring better wettability and antioxidant properties, respectively. However, the coatings on the lenses may interfere with their optical properties since the power depends on the lens radius and water content. In this work, the sonochemical process and the generated coating did not alter the dry nominal dioptric power (PWR_d) of the CL (Fig 1A). The difference in PWR_d of coated CL compared to control was lower than the ± 0.25 D - tolerance limit indicated in the ISO 18369-3:2017. On the other hand, the equilibrium water content of CL remained invariable after the sonochemical treatment (Fig 1B). The amount of coating was too small to influence the water content of the CL (Sec. 3.5). The invariable water content and PWR_d pointed out that CL maintained their geometry and refractive properties [41]. On the other hand, the reduction of the surface hydrophobicity of silicone hydrogel CL has been the main driving force for the evolution of these optical devices [42,43]. Comfilcon A material is the main component of our CL that are the III generation silicone hydrogel CL, and was developed using long silicone chains with OH-groups in order to avoid additional surface treatments previously required for improving the wettability of the I generation silicone hydrogel CL [44]. The coatings containing CS present lower WCA, e.g. higher surface hydrophilicity (Fig. 1C) than those without CS as anticipated by the high hydrophilicity of CS [27]. The high hydrophilicity (low WCA) of the ternary coating was a result of the surface enrichment of the CL with the amino and hydroxyl functional groups of CS and the hydroxyl and carboxylic groups of GA contributing to the establishment of hydrogen bonds with water [41,45].

Con formato: Fuente: 10 pto
Con formato: Fuente: 10 pto
Con formato: Fuente: 10 pto
Con formato: Fuente: 10 pto
Con formato: Fuente: 10 pto
Con formato: Fuente: 10 pto
Con formato: Fuente: 10 pto
Con formato: Fuente: 10 pto
Con formato: Fuente: 10 pto
Con formato: Fuente: 10 pto
Con formato: Fuente: 10 pto
Con formato: Fuente: 10 pto

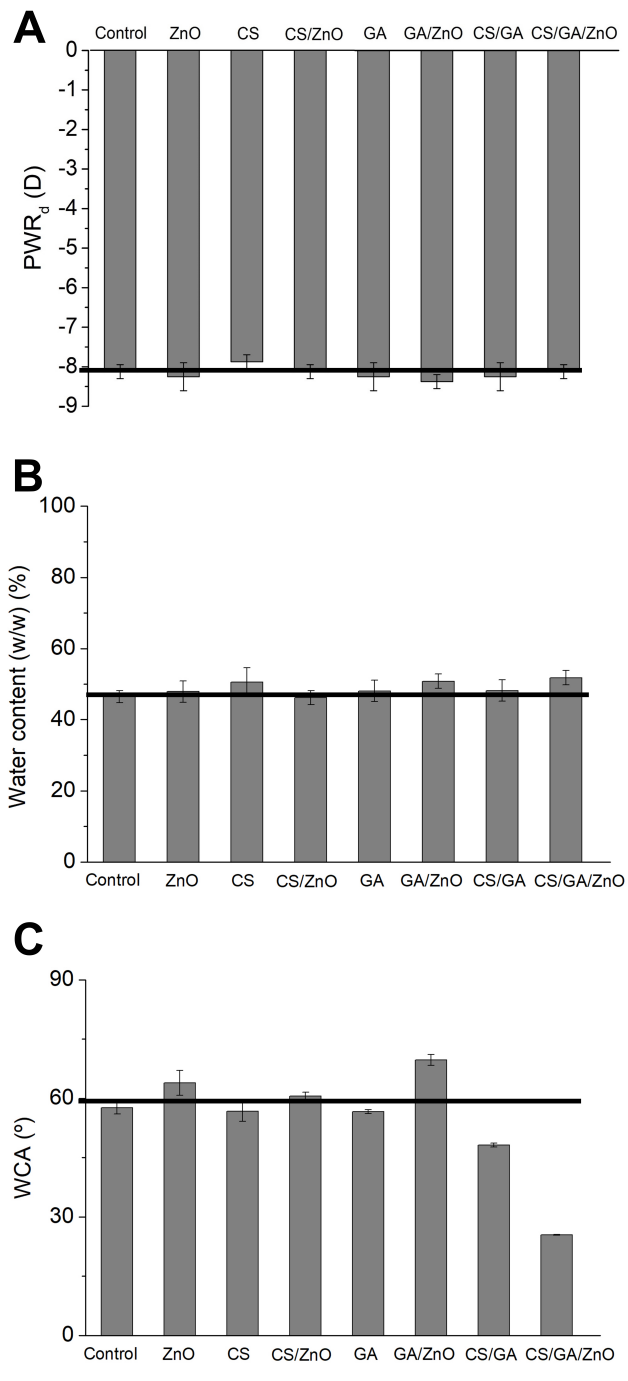

Figure 1. A) Dry dioptric power, B) water content and C) water contact angle of CL after the sonochemical coating.

3.2 Antioxidant activity

All GA functionalized CL showed similar DPPH scavenging abilities. Up to 95 % DPPH inhibition was achieved (Fig 2), due to the saturation of the liquid medium with sufficient amount of polyphenols. The presence of other compounds in the hybrid coatings did not affect the GA antioxidant activity. High antioxidant activity of the coatings would help the innate antioxidant defense system of cornea to face the oxidative stress generated by the formation of ROS [46] thus reducing the pathogenesis of ROS-associated eye diseases [29–31].

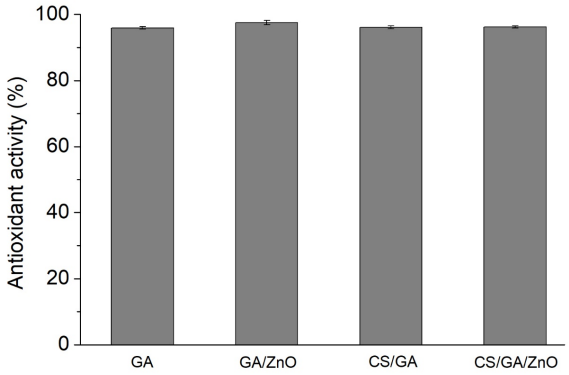

Figure 2. Antioxidant activity of CL after the sonochemical functionalization with GA containing coatings.

3.3 Antibacterial activity

The antibacterial properties of ZnO NPs, CS and GA used for coating of CL have been reported previously [25,47,48]. However, the antibacterial potential of sonochemically-generated nanocomposite coatings of the three bioactives are not studied yet. In this study, we assessed the antibacterial efficiency of the NP-coated CL against *S. aureus* (Fig. 3), which is associated with CL-related eye conditions, such as MK, IK, CLARE and CLPU [1].

Coatings containing GA demonstrated the highest antibacterial efficiency, which is correlated with the prevalent GA content [48]. Moreover, the individual ZnO NPs coating provided also strong bactericidal activity as expected [15,49,50]. The ternary hybrid coating composed of ZnO NPs, CS and GA shares the highest antibacterial efficiency (Fig. 3), achieving more than 4.5 logs reduction of bacterial viability.

Con formato: Fuente: 10 pto
Con formato: Fuente: 10 pto
Con formato: Fuente: 10 pto
Con formato: Fuente: 10 pto
Con formato: Fuente: 10 pto
Con formato: Fuente: 10 pto
Con formato: Fuente: 10 pto
Con formato: Fuente: 10 pto
Con formato: Fuente: 10 pto
Con formato: Fuente: 10 pto
Con formato: Fuente: 10 pto

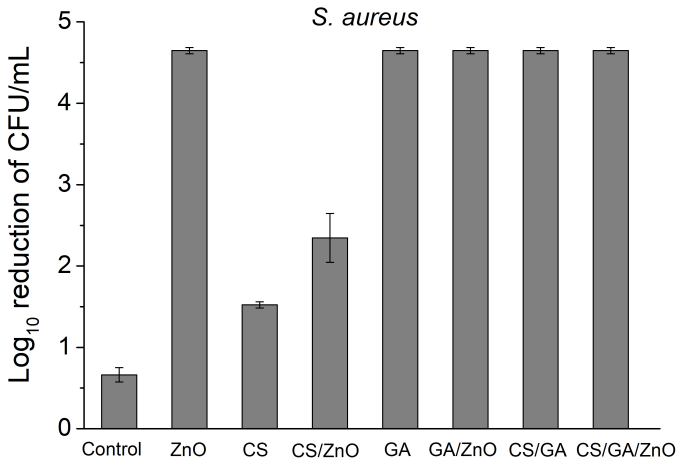

Figure 3. Antibacterial activity of CL after 24 h of contact with *S. aureus*.

3.4 Biocompatibility assay

GA and CS are natural non-toxic compounds, whereas ZnO NPs have shown reduced biocompatibility to mammalian cells [51] despite their extended use in cosmetics and sun protection creams [52]. The antibacterial effect of ZnO NPs comprises the ROS formation [18] that besides being harmful for bacteria may affect significantly the viability of the human cells. The toxicity tests (Fig. 4) with fibroblast and keratinocyte cell lines revealed high cell viability (70 - 100 %) for all CS containing coatings as expected due to its previously demonstrated biocompatibility [53]. However, lower cells viability was observed in the case of GA based composite coatings, in particular the individual GA material, where probably the high GA concentration and lower coating stability in aqueous medium led to the burst GA release and cells death within the 24 h of exposure [54]. In contrast, the ZnO NPs - coatings presented good biocompatibility, due to the low amount of NPs used [55] for the CL functionalization. Importantly, the ternary hybrid nanocomposite coating showed good biocompatibility - 93 and 72 % of fibroblasts and keratinocytes cells were viable, respectively.

Con formato: Fuente: 10 pto
Con formato: Fuente: 10 pto
Con formato: Fuente: 10 pto
Con formato: Fuente: 10 pto
Con formato: Fuente: 10 pto
Con formato: Fuente: 10 pto
Con formato: Fuente: 10 pto
Con formato: Fuente: 10 pto
Con formato: Fuente: 10 pto
Con formato: Fuente: 10 pto
Con formato: Fuente: 10 pto

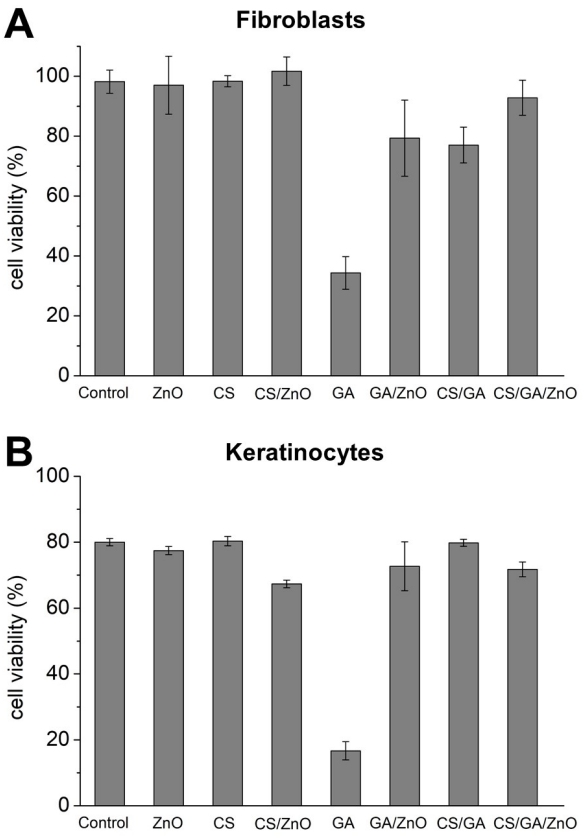

Figure 4. Viability of human A) fibroblasts and B) keratinocytes cell lines after 24 h of contact with the sonochemically functionalized CL.

3.5 Hybrid CS/GA/ZnO CL coating characterization

As expected the hybrid nanocomposite coating led to multiple benefits as enhanced biocompatibility (Fig 4), strong antibacterial activity against common ocular pathogen (Fig 3), high antioxidant effect (Fig 2) and improved wettability (Fig 1C). Therefore, the surface morphology and topography of the CS/GA/ZnO NPs CL was further analysed by SEM and AFM. The AFM images revealed a uniform surface of pristine CL with no relevant structures observed (Fig. 5A) and low surface roughness as previously observed for Comfilcon A CL [56,57]. In contrast, nanoscale irregularities were observed on the coated CL (Fig. 5B). The dark and light shades on the AFM images correspond respectively to the CL surface and the coating. Coated CL presented bright protuberances of 92.5 ± 47.5 nm that are related to the deposition of the hybrid CS/GA/ZnO coating. The root mean square roughness (Rq) assessed from the AFM images was 55.8 nm, confirming the surface nanostructuring of the sonochemically coated CL. Furthermore, the nanometric height of the coatings correlates with the invariable water content (Fig 1B) and shows that the CL structure is negligibly modified. The coatings onto the CL surface were probably physically embedded [32] via the high energy US, as previously observed for a number of US functionalized materials and surfaces [28,32,33].

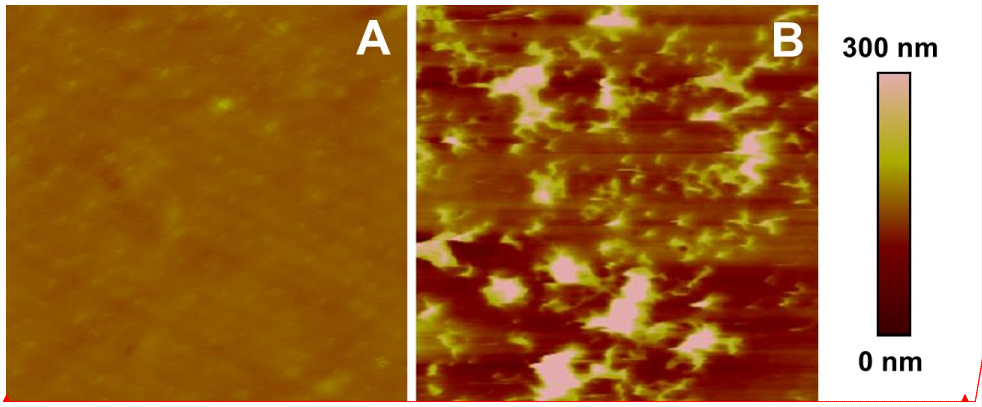

Figure 5. Topographic images of the surface of: A) pristine CL and B) CS/GA/ZnO coated CL. Scanned area: 5 × 5 μm^2.

The pristine CL surface presents no relevant surface microstructures (Fig 6A) when imaged in SEM, whereas the coated CL (Fig 6B) presents needle shaped structures with size ~ 1 µm. The EDS analysis further confirmed the presence of Zn in the coated CL.

Con formato: Fuente: 10 pto
Con formato: Fuente: 10 pto
Con formato: Fuente: 10 pto
Con formato: Fuente: 10 pto
Con formato: Fuente: 10 pto
Con formato: Fuente: 10 pto
Con formato: Fuente: 10 pto
Con formato: Fuente: 10 pto

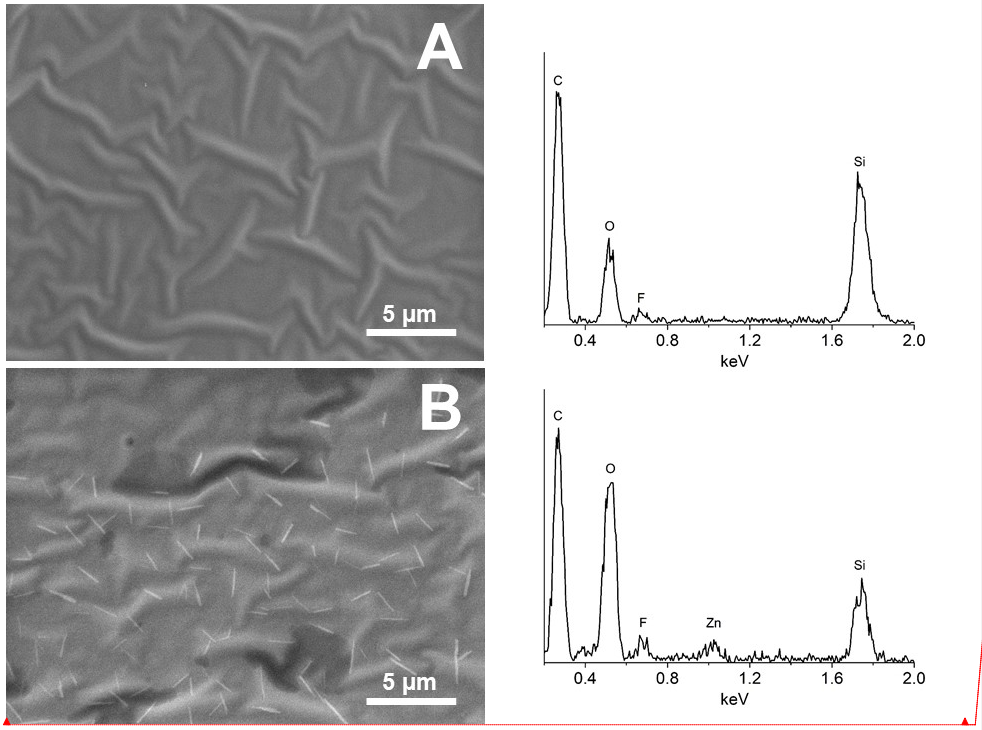

Figure 6. SEM images of CL and EDS spectrum showing the composition of pristine CL (A) and CS/GA/ZnO coated CL (B).

The amount of each compound of the ternary coated CL was further determined. The coated CL had 2.16 ± 0.75 µg of Zn, 2.72 ± 0.78 µg of CS and 0.93 ± 0.1 mg of GA. The use of the CS, GA and ZnO NPs with different antibacterial modes of action defines the high antibacterial potential of the hybrid CLs while at the same time diminishes the side effects to human cells (Fig 4). Phenolic compounds possess strong antibacterial activity as result of membrane destabilisation, inhibition of nucleic acids synthesis and inactivation of essential for bacteria enzymes [48] whereas amino-bearing polymers are able to interact electrostatically with bacterial cell and disturb its membrane [25]. Therefore, GA and CS together in the CL coatings could destabilize bacterial membrane and potentiate the antibacterial action of ZnO NPs. The ZnO dissolution to Zn^{2+} and the subsequent ROS generation would then lead to cellular proteins and DNA damage [18,19]. The utilization of small sized ZnO NPs (< 40 nm) with high surface area to volume ratio would lead to the increased formation of $Zn^{2+,}$ favouring their killing potential [40,55,58]. From other side, the visible light exposure upon wearing the ZnO NPs coated CL would also enhance their bactericidal efficacy [58] while maintaining unaffected the optical properties of the CL. Despite the

Con formato: Fuente: 10 pto
Con formato: Fuente: 10 pto
Con formato: Fuente: 10 pto
Con formato: Fuente: 10 pto
Con formato: Fuente: 10 pto
Con formato: Fuente: 10 pto
Con formato: Fuente: 10 pto
Con formato: Fuente: 10 pto
Con formato: Fuente: 10 pto
Con formato: Fuente: 10 pto
Con formato: Fuente: 10 pto
Con formato: Fuente: 10 pto

bactericidal activity, the hydrophilic character of the ternary hybrid coating will additionally enhance the CL wearing comfort inhibiting the attachment of proteins and bacterial cells [59].

Nevertheless, the strong antibacterial activity, the biocompatibility of the hybrid coatings is the most critical parameter for their final medical application. Herein, we could successfully design effective antibacterial and antioxidant composite coatings of ZnO NPs, CS and GA, which do not induce human cells damage. The amount of ZnO NPs embedded in the coating is significantly lower than the previously determined toxic concentrations in *in vivo* studies with rats. Damage of eye retina (retinopathy) was observed in the rats treated with ZnO NPs at concentrations between 250 and 500 mg of ZnO NPs/kg [60,61]. The authors were however unable to discern if this effect was due to the ZnO NPs themselves or to the release of Zn^{2+} ions [61]. Oppositely, Zn^{2+} at concentration below 100µM were able to prevent retinal ischemia when administrated [60]. The presence of antioxidant GA at non-toxic concentrations would scavenge the free oxygen radicals and therefore reduce the ocular oxidative stress implicated in the pathogenesis of numerous eye diseases [29]. Recent studies have defined the 10 % (w/v) concentration of polyphenols [59] as the limit for treatment without causing irritation in the eyes. These values are far below of the amount 0.3 % (w/v) we have used in our antioxidant hybrid coatings. The combination of ZnO NPs with the biocompatible CS and GA resulted in the generation of safe and efficient hybrid coating, which would also protect the eye from ROS damage. Moreover, the multi-action antimicrobial mechanism would make the development of resistance less unlikely, because multiple simultaneous gene mutations in the same bacterial cell would be required [64].

Con formato: Fuente: 10 pto

Con formato: Fuente: 10 pto

Con formato: Fuente: 10 pto

Con formato: Fuente: 10 pto

4. CONCLUSIONS

Multifunctional coatings containing of ZnO NPs, CS and GA were engineered on CL in a one-step sonochemical process. High intensity US embeds the three compounds onto CL maintaining at the same time invariable the geometry and refractive properties of CL. The hybrid CS/GA/ZnO coating improved the surface wettability and antioxidant activity by 95 % of the CL, which could be correlated with an increase in the CL wearing comfort. The ternary hybrid coating couples high antibacterial efficiency (> 4.5 logs reduction) towards the main bacteria causing CL-related conditions, with high biocompatibility to human cells. The sonochemical approach showed to be an efficient fast, simple and reproducible method for surface nano-functionalization of CL, without altering their geometry and refractive properties.

AUTHOR INFORMATION

*Corresponding author: Dr. Tzanko Tzanov, tel.: +34 93 739 85 70, fax: +34 93 739 82 25, e-mail: tzanko.tzanov@upc.edu

NOTES

The authors declare no competing financial interest.

ACKNOWLEDGEMENTS

The research leading to these results has received funding from European Community's Horizon 2020 Framework Program H2020 (H2020-720851 project PROTECT - Pre-commercial lines for production of surface nanostructured antimicrobial and anti-biofilm textiles, medical devices and water treatment membranes).

References

[1] D. Dutta, M.D.P. Willcox, Antimicrobial contact lenses and lens cases: A review, Eye Contact Lens. 40 (2014) 312–324. doi:10.1097/ICL.0000000000000056.

[2] P. Ramamoorthy, L.T. Sinnott, J.J. Nichols, Treatment, Material, Care, and Patient-related Factors in Contact Lens-Related Dry Eye, Optom Vis Sci. 85 (2008) 764–772.

[3] X.H. Hu, H.P. Tan, D. Li, M.Y. Gu, Surface functionalisation of contact lenses by CS / HA multilayer film to improve its properties and deliver drugs, Mater. Technol. Adv. Perform. Mater. 29 (2014) 8–13. doi:10.1179/1753555713Y.0000000063.

[4] H. Shin, K. Price, L. Albert, J. Dodick, L. Park, G. Dominguez-bello, Changes in the Eye Microbiota Associated with Contact Lens Wearing, MBio. 7 (2016) 1–6. doi:10.1128/mBio.00198-16.Editor.

[5] L. Keay, K. Edwards, T. Naduvilath, H.R. Taylor, G.R. Snibson, K. Forde, F. Stapleton, Microbial keratitis: Predisposing factors and morbidity, Ophthalmology. 113 (2006) 109–116. doi:10.1016/j.ophtha.2005.08.013.

[6] L.B. Szczotka-Flynn, E. Pearlman, M. Ghannoum, Microbial contamination of contact lenses, lens care solutions, and their accessories: A literature review, Eye Contact Lens. 36 (2010) 116–129. doi:10.1097/ICL.0b013e3181d20cae.

[7] I. Jalbert, M.D.P. Willcox, D.F. Sweeney, Isolation of Staphylococcus aureus from a contact lens at the time of a contact lens-induced peripheral ulcer: Case report, Cornea. 19 (2000) 116–120. doi:10.1097/00003226-200001000-00023.

[8] K. Ivanova, E. Ramon, J. Hoyo, T. Tzanov, Innovative Approaches for Controlling Clinically Relevant Biofilms, Curr. Trends Futur. Prospect. 17 (2017) 1889–1914. doi:10.2174/1568026617666170105143315.

[9] D. Dutta, A.K. Vijay, N. Kumar, M.D.P. Willcox, Melimine-coated antimicrobial contact lenses reduce microbial keratitis in an animal model, Investig. Ophthalmol. Vis. Sci. 57 (2016) 5616–5624. doi:10.1167/iovs.16-19882.

[10] H. Jenssen, P. Hamill, R.E.W. Hancock, Peptide antimicrobial agents, Clin. Microbiol. Rev. 19 (2006) 491–511. doi:10.1128/CMR.00056-05.

[11] B.M.K. Bandara, P.R. Sankaridurg, M.D.P. Willcox, Non-steroidal anti inflammatory agents decrease bacterial colonisation of contact lenses and prevent adhesion to human corneal epithelial

Con formato: Fuente: 10 pto

cells, Curr. Eye Res. 29 (2004) 245–251. doi:10.1080/02713680490516729.

[12] F.W. Fraunfelder, Corneal toxicity from topical ocular and systemic medications, Cornea. 25 (2006) 1133–1138. doi:10.1097/01.ico.0000240084.27663.fd.

[13] M. George, G. Pierce, M. Gabriel, C. Morris, D. Ahearn, Effects of quorum sensing molecules of Pseudomonas aeruginosa on organism growth, elastase B production, and primary adhesion to hydrogel contact lenses, Eye Contact Lens. 31 (2005) 54–61. doi:10.1097/01.ICL.0000146324.28865.E8.

[14] O. Bondarenko, K. Juganson, A. Ivask, K. Kasemets, M. Mortimer, A. Kahru, Toxicity of Ag, CuO and ZnO nanoparticles to selected environmentally relevant test organisms and mammalian cells in vitro: A critical review, Arch. Toxicol. 87 (2013) 1181–1200. doi:10.1007/s00204-013-1079-4.

[15] H. Yang, C. Liu, D. Yang, H. Zhang, Z. Xi, Comparative study of cytotoxicity, oxidative stress and genotoxicity induced by four typical nanomaterials: the role of particle size, shape and composition, J. Appl. Toxicol. 29 (2009) 69–78. doi:10.1002/jat.1385.

[16] S.A. Khan, F. Noreen, S. Kanwal, A. Iqbal, G. Hussain, Green synthesis of ZnO and Cu-doped ZnO nanoparticles from leaf extracts of Abutilon indicum, Clerodendrum infortunatum, Clerodendrum inerme and investigation of their biological and photocatalytic activities, Mater. Sci. Eng. C. 82 (2018) 46–59. doi:10.1016/j.msec.2017.08.071.

[17] S.A. Khan, F. Noreen, S. Kanwal, G. Hussain, Comparative synthesis, characterization of Cu-doped ZnO nanoparticles and their antioxidant, antibacterial, antifungal and photocatalytic dye degradation activities, Dig. J. Nanomater. Biostructures. 12 (2017) 877–889. doi:http://www.chalcogen.ro/877_KhanSA.pdf.

[18] A. Nel, L. Mädler, D. Velegol, T. Xia, E.M. V Hoek, P. Somasundaran, F. Klaessig, V. Castranova, M. Thompson, Understanding biophysicochemical interactions at the nano-bio interface, Nat. Mater. 8 (2009) 543–557. doi:10.1038/nmat2442.

[19] A. Nel, T. Xia, L. Mädler, N. Li, Toxic Potential of Materials at the Nanolevel, Science (80-.). 311 (2006) 622–627. doi:10.1126/science.1114397.

[20] M. Guillon, L. McGrogan, J.P. Guillon, E. Styles, C. Maissa, Effect of material ionicity on the performance of daily disposable contact lenses., Contact Lens Anterior Eye. 20 (1997) 3–8. doi:10.1016/S1367-0484(97)80029-X.

[21] C. Riley, G. Young, R. Chalmers, Prevalence of ocular surface symptoms, signs, and uncomfortable hours of wear in contact lens wearers: The effect of refitting with daily-wear silicone hydrogel lenses (senofilcon A), Eye Contact Lens. 32 (2006) 281–286. doi:10.1097/01.icl.0000224522.04723.7a.

[22] B.J. Mondino, S.M. Salamon, G.W. Zaidman, Allergic and toxic reactions in soft contact lens wearers, Surv. Ophthalmol. 26 (1982) 337–344. doi:10.1016/0039-6257(82)90126-6.

[23] H. Thissen, T. Gengenbach, R. du Toit, D.F. Sweeney, P. Kingshott, H.J. Griesser, L. Meagher, Clinical observations of biofouling on PEO coated silicone hydrogel contact lenses, Biomaterials. 31 (2010) 5510–5519. doi:10.1016/j.biomaterials.2010.03.040.

[24] A. Singh, P. Li, V. Beachley, P. Mcdonnell, J.H. Elisseeff, A hyaluronic acid-binding contact lens with enhanced water retention, Contact Lens Anterior Eye. 38 (2015) 79–84. doi:10.1016/j.clae.2014.09.002.

[25] J. Champer, J. Patel, N. Fernando, E. Salehi, V. Wong, J. Kim, Chitosan against cutaneous pathogens., AMB Express. 3 (2013) 37. doi:10.1186/2191-0855-3-37.

[26] S. Boributh, A. Chanachai, R. Jiraratananon, Modification of PVDF membrane by chitosan solution for reducing protein fouling, J. Memb. Sci. 342 (2009) 97–104. doi:10.1016/j.memsci.2009.06.022.

[27] Z.W. Dai, F.Q. Nie, Z.K. Xu, Acrylonitrile-based copolymer membranes containing reactive groups: Fabrication dual-layer biomimetic membranes by the immobilization of biomacromolecules, J. Memb. Sci. 264 (2005) 20–26. doi:10.1016/j.memsci.2005.04.022.

[28] M. Salat, P. Petkova, J. Hoyo, I. Perelshtein, A. Gedanken, T. Tzanov, Durable antimicrobial cotton textiles coated sonochemically with ZnO nanoparticles embedded in an in-situ enzymatically generated bioadhesive, Carbohydr. Polym. 189 (2018) 198–203. doi:10.1016/j.carbpol.2018.02.033.

[29] Y. Chen, G. Mehta, V. Vasiliou, Antioxidant defenses in the ocular surface, Ocul. Surf. 7 (2009) 176–185. doi:10.1016/S1542-0124(12)70185-4.

[30] M. Chwa, S.R. Atilano, V. Reddy, N. Jordan, D.W. Kim, M.C. Kenney, Increased stress-induced generation of reactive oxygen species and apoptosis in human keratoconus fibroblasts, Investig. Ophthalmol. Vis. Sci. 47 (2006) 1902–1910. doi:10.1167/iovs.05-0828.

[31] S. Nakamura, M. Shibuya, H. Nakashima, R. Hisamura, N. Masuda, T. Imagawa, M. Uehara, K.

Tsubota, Involvement of oxidative stress on corneal epithelial alterations in a blink-suppressed dry eye, Investig. Ophthalmol. Vis. Sci. 48 (2007) 1552–1558. doi:10.1167/iovs.06-1027.

[32] R. Gottesman, S. Shukla, N. Perkas, L.A. Solovyov, Y. Nitzan, A. Gedanken, Sonochemical Coating of Paper by Microbiocidal Silver Nanoparticles, 27 (2011) 720–726. doi:10.1021/la103401z.

[33] J.G. Martinez Colunga, S. Sánchez-Valdes, L.F. Ramos-deValle, M.C. Ibarra-alonso, T. Lozano-ramirez, P.G. Lafleur, Simultaneous Polypropylene Functionalization and Nanoclay Dispersion in PP / Clay Nanocomposites using Ultrasound, J. Appl. Polym. Sci. Polym. Sci. 40631 (2014) 1–8. doi:10.1002/app.40631.

[34] R.S. Davidson, A. Safdar, J.D. Spencer, B. Robinson, Applications of ultrasound to materials chemistry, Ultrasonics. 29 (1999) 295–236. doi:10.1016/0041-624X(87)90009-6.

[35] D. Radziuk, H. Möhwald, Ultrasonically treated liquid interfaces for progress in cleaning and separation processes, Phys. Chem. Chem. Phys. 18 (2016) 21–46. doi:10.1039/C5CP05142H.

[36] H.A. Ketelson, D.L. Meadows, R.P. Stone, Dynamic wettability properties of a soft contact lens hydrogel, Colloids Surfaces B Biointerfaces. 40 (2005) 1–9. doi:10.1016/j.colsurfb.2004.07.010.

[37] I. Stefanov, S. Pérez-Rafael, J. Hoyo, J. Cailloux, O.O. Santana Pérez, D. Hinojosa-Caballero, T. Tzanov, Multifunctional Enzymatically Generated Hydrogels for Chronic Wound Application, Biomacromolecules. 18 (2017) 1544–1555. doi:10.1021/acs.biomac.7b00111.

[38] A. Francesko, K. Ivanova, J. Hoyo, S. Pérez-Rafael, P. Petkova, M.M. Fernandes, T. Heinze, E. Mendoza, T. Tzanov, Bottom-up Layer-by-Layer Assembling of Antibacterial Freestanding Nanobiocomposite Films, Biomacromolecules. 19 (2018) 3628–3636. doi:10.1021/acs.biomac.8b00626.

[39] Perelshtein, N. Perkas, A. Gedanken, Ultrasonic coating of textiles by antibacterial and antibiofilm nanoparticles, in: M. Ashokkumar (Ed.), Handb. Ultrason. Sonochemistry, Springer Science, 2015: pp. 1–29. doi:10.1007/978-981-287-470-2.

[40] A. Sirelkhatim, S. Mahmud, A. Seeni, N.H.M. Kaus, L.C. Ann, S.K.M. Bakhori, H. Hasan, D. Mohamad, Review on zinc oxide nanoparticles: Antibacterial activity and toxicity mechanism, Nano-Micro Lett. 7 (2015) 219–242. doi:10.1007/s40820-015-0040-x.

[41] P. Monti, R. Simonib, The role of water in the molecular structure and properties of soft contact lenses and surface interactions, J. Mol. Struct. 269 (1992) 243–255.

[42] B.J. Tighe, A decade of silicone hydrogel development: Surface properties, mechanical properties, and ocular compatibility, Eye Contact Lens. 39 (2013) 4–12. doi:10.1097/ICL.0b013e318275452b.

[43] J.T. Jacob, Biocompatibility in the development of silicone-hydrogel lenses, Eye Contact Lens. 39 (2013) 13–19. doi:10.1097/ICL.0b013e31827dbb00.

[44] R. Brygoła, S. Sęk, M. Sokołowski, M. Kowalczyk-Hernández, J. Pniewski, Limits in measurements of contact lens surface profile using atomic force microscopy, Colloids Surfaces B Biointerfaces. 165 (2018) 229–234. doi:10.1016/j.colsurfb.2018.02.018.

[45] J. Lamarra, L. Giannuzzi, S. Rivero, A. Pinotti, Assembly of chitosan support matrix with gallic acid-functionalized nanoparticles, Mater. Sci. Eng. C. 79 (2017) 848–859. doi:10.1016/j.msec.2017.05.104.

[46] V. Pastori, S. Tavazzi, M. Lecchi, Lactoferrin - Loaded Contact Lenses : Eye Protection Against Oxidative Stress, 34 (2015) 693–697. doi:10.1097/ICO.0000000000000435.

[47] S. Stankic, S. Suman, F. Haque, J. Vidic, Pure and multi metal oxide nanoparticles: synthesis, antibacterial and cytotoxic properties, J. Nanobiotechnology. 14 (2016) 73. doi:10.1186/s12951-016-0225-6.

[48] A. Borges, C. Ferreira, M.J. Saavedra, M. Simões, Antibacterial activity and mode of action of ferulic and gallic acids against pathogenic bacteria., Microb. Drug Resist. 19 (2013) 256–65. doi:10.1089/mdr.2012.0244.

[49] S.A. Khan, S. Shahid, S. Jabin, S. Zaman, M.N. Sarwar, Synthesis and characterization of un-doped and copperdoped zinc oxide nanoparticles for their optical and antibacterial studies, Dig. J. Nanomater. Biostructures. 13 (2018) 285–297. doi:10.3390/molecules22122242.

[50] S.A. Khan, F. Noreen, S. Kanwal, A. Iqbal, G. Hussain, Green synthesis of ZnO and Cu-doped ZnO nanoparticles from leaf extracts of Abutilon indicum, Clerodendrum infortunatum, Clerodendrum inerme and investigation of their biological and photocatalytic activities, Mater. Sci. Eng. C. 82 (2018) 46–59. doi:10.1016/j.msec.2017.08.071.

[51] E. Demir, H. Akça, B. Kaya, D. Burgucu, O. Tokgün, F. Turna, S. Aksakal, G. Vales, A. Creus, R. Marcos, Zinc oxide nanoparticles: Genotoxicity, interactions with UV-light and cell-transforming potential, J. Hazard. Mater. 264 (2014) 420–429. doi:http://dx.doi.org/10.1016/j.jhazmat.2013.11.043.

[52] Y.-N. Chang, M. Zhang, L. Xia, J. Zhang, G. Xing, The Toxic Effects and Mechanisms of CuO and ZnO Nanoparticles, Materials (Basel). 5 (2012) 2850–2871. doi:10.3390/ma5122850.

[53] P.J. Vandevord, H.W.T. Matthew, S.P. Desilva, L. Mayton, B. Wu, P.H. Wooley, Evaluation of the biocompatibility of a chitosan scaffold in mice, J Biomed Mater Res. 5 (n.d.) 585–590. doi:10.1002/jbm.1270.

[54] D.J. Yang, S.H. Moh, D.H. Son, S. You, A.W. Kinyua, C.M. Ko, M. Song, J. Yeo, Y.H. Choi, K.W. Kim, Gallic Acid Promotes Wound Healing in Normal and Hyperglucidic Conditions, Molecules. 21 (2016) 1–15. doi:10.3390/molecules21070899.

[55] W. Song, J.J. Zhang, J. Guo, J.J. Zhang, F. Ding, L. Li, Z. Sun, Role of the dissolved zinc ion and reactive oxygen species in cytotoxicity of ZnO nanoparticles, Toxicol. Lett. 199 (2010) 389–397. doi:10.1016/j.toxlet.2010.10.003.

[56] J.M. González-Méijome, A. Löpez-Alemany, J.B. Almeida, M.A. Parafita, Surface AFM microscopy of unworn and worn samples of silicone hydrogel contact lenses, J. Biomed. Mater. Res. - Part B Appl. Biomater. 88 (2009) 75–82. doi:10.1002/jbm.b.31153.

[57] M.J. Giraldez, C. Serra, M. Lira, M.E.C.D. Real Oliveira, E. Yebra-Pimentel, Soft contact lens surface profile by atomic force microscopy, Optom. Vis. Sci. 87 (2010). doi:10.1097/OPX.0b013e3181e170c5.

[58] N. Jones, B. Ray, K.T. Ranjit, A.C. Manna, Antibacterial activity of ZnO nanoparticle suspensions on a broad spectrum of microorganisms, FEMS Microbiol. Lett. 279 (2008) 71–76. doi:10.1111/j.1574-6968.2007.01012.x.

[59] H. Tang, T. Cao, X. Liang, A. Wang, S.O. Salley, J. McAllister, K.Y.S. Ng, Influence of silicone surface roughness and hydrophobicity on adhesion and colonization of Staphylococcus epidermidis, J. Biomed. Mater. Res. - Part A. 88 (2009) 454–463. doi:10.1002/jbm.a.31788.

[60] M. Ugarte, N.N. Osborne, Zinc in the retina, Prog. Neurobiol. 64 (2001) 219–249. doi:10.1016/S0301-0082(00)00057-5.